

>5% Compressive Strain in Graphene via the Self-Rolled-up Membrane Platform

Paul Froeter,¹ Parsian K. Mohseni,^{1,2} Apratim Khandelwal,¹ and Xiuling Li^{1,2*}

¹Department of Electrical and Computer Engineering, University of Illinois, Urbana, IL 61801

²Current address: Department of Electrical and Computer Engineering, Rochester Institute of Technology, Rochester, NY 14623

³Department of Electrical and Computer Engineering, University of Texas, Austin, TX 78738

*Corresponding author: Xiuling.li@utexas.edu

Abstract

Graphene is an atomically thin metallic membrane capable of sustaining reversible strain and offers a tempting prospect of controlling its optoelectronic properties via strain. Graphene's exceptional mechanical flexibility (Young's modulus) and tensile strength provide a lot of room for strain engineering. Here we use the self-rolled-up membrane (S-RuM) platform for strain engineering and integration of graphene with stressed dielectric (e.g. SiN_x) thin films. Graphene rolls up or down together with the stressed film upon releasing from the substrate and the curvature of the rolled-up film stack enables the strain tuning of the graphene monolayer. Raman spectroscopy was used to characterize the uniaxial strain in rolled-up graphene by quantifying the red-shift and splitting of the G peak (G⁺ and G⁻) in the doubly degenerate E_{2g} optical mode. ~5% compressive strain is realized using a S-RuM diameter of ~ 2 μm. By reducing the diameter of the S-RuM structure, even higher strain level can be reached. The S-RuM approach can also be readily applied to induce strain in other materials beyond the level that can be achieved using conventional approaches.

Introduction

Graphene is a 2D sheet of sp² hybridized carbon atoms arranged in a honeycomb lattice. Since its discovery it has attracted a lot of attention due to its unique mechanical, electrical and optical properties [1–3]. Moreover, the atomically thin nature of graphene provides several knobs to tune its properties based on the required application. One such unique knob is the use of long-range strains to tune its opto-electronic properties like carrier density, band gap and work function [3–6]. Modulation of such effects has been studied in great detail by both first-principles calculations and experiments [7–9]. While most experimental techniques have introduced platforms that can

study either one or two such effects individually, here-in we show that our platform can be used to study multiple effects simultaneously. Due to lattice mismatch [10] or the substrate roughness [11,12], strains are expected to arise naturally in graphene. However, there are several ways to intentionally induce and control uniaxial [7,13,14] and biaxial [9,15] strain in graphene. Most of the techniques involve complex fabrication procedures and thus suffer from degraded graphene quality hindering the observation of strain effects. Here we report a simple strain tuning method by using SiN_x stressed thin films as a scaffold to support and apply strain to CVD grown graphene monolayers.

In the past, a variety of material combinations including semiconductors [16,17], oxides [18], nitrides [19], metals [20] polymers [21] and other hybrid thin films [22]17,36 have been rolled-up into micro or nanotubes, scrolls, pockets and helical structures. These structures are formed by spontaneous deformation of stressed thin films driven by relaxation of strain energy. These self-rolled-up membranes (S-RuM), first discovered by Prinz et al in 2000, have proven to be an excellent platform for various on-chip and off-chip applications in electronics, optics, materials science, biology and micro/nanofluidics [23–25]. The overarching physical principle of S-RuMs is strain-driven spontaneous deformation of thin-film membranes into a cylindrical form factor. The membranes can be released from their substrates to self-assemble into tubes, coils, rings or helices depending upon the initial 2D geometry of the patterned nanomembrane. These membranes can be rolled-up by combining standard lithography and etching processes. Most rolling mechanisms are based on the use of a sacrificial layer that can be etched via a selective dry etch [26] or wet-etch [27] process. In this study, we used a wet-etch process to achieve a controlled release of the 2D pattern (graphene/SiN_x) to serially tune the uniaxial strain in the CVD grown monolayer graphene. The diameter of the resulting microtubular structure is linked directly to the strain accumulated in the graphene and Raman spectroscopy is used to study the imposition of the uniaxial strain.

Experimental

Monolayer graphene films are grown through the Cu-catalyzed chemical vapor deposition (CVD) technique, followed by direct deposition, via the well-established poly(methyl-methacrylate) (PMMA) transfer process [28], onto strained bilayer stacks of SiN_x. Upon photo-lithographic definition of rectangular pads and wet-etching of an underlying sacrificial layer, an inherent strain differential arising within the bilayer stack of low- and high-frequency plasma-enhanced chemical vapor deposition (PECVD)-formed SiN_x films causes the spontaneous rolling of micro-tubular structures [19]. Thus, the deposited graphene film is subjected to uniaxial compression upon release of the inherently strained SiN_x membrane. The degree of strain applied to the SiN_x stack and, therefore, that which is induced in the graphene sheet, is a function of the micro-tube diameter, and is directly tuned according to the relative thickness of the low- and high-frequency deposited

nitride layers. Alternatively, the diameter of the micro-tubes can be controlled through partial or full etching of the underlying sacrificial layer.

Results and Discussions

Figure 1 shows tilted-view scanning electron microscopy (SEM) images of flat, partially released, and fully rolled graphene films on or in SiN_x microtubes.

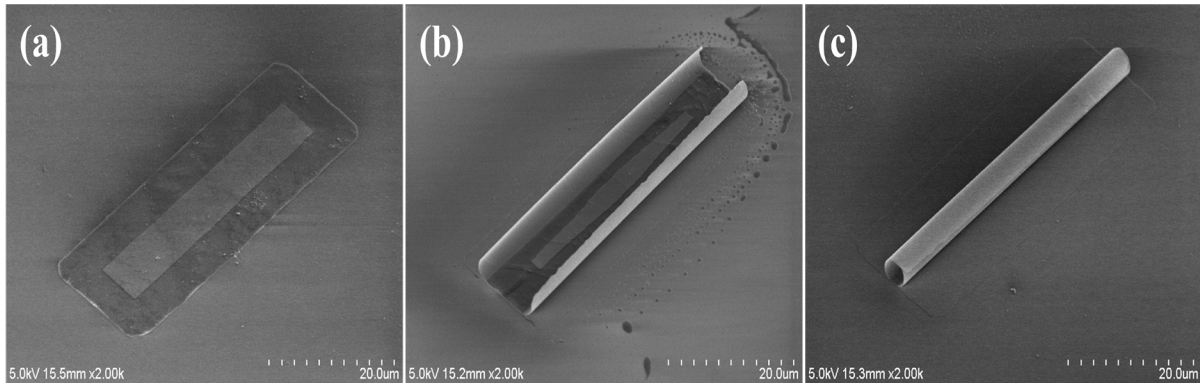


Figure 1. 45° tilted-view SEM images of (a) un-rolled, (b) partially rolled, and (c) fully rolled graphene/SiN_x micro-tube. The graphene film is situated on top of the flat (unreleased) pad, as shown in (a). However, as the microtube begins to roll-up, the graphene film becomes compressively strained and contorts in tandem with, and inside, the microtube structure, as shown in (b) and (c).

Multi-diameter chips (MDC) are very useful for this type of strain analysis as they provide a larger range of results from a single sheet of graphene, improving the accuracy of batch characterization runs. These MDC consist of a varying thickness compressive or tensile layer and multiple photolithography patterning steps, shown in Figure 2. This multi-step deposition process is guided by the equation relating bending radius to film parameters and supported in our investigation. In our experiments Mg was used as the sacrificial layer, due to its ability to act as an etch stop in CF₄-based plasma, which is commonly used to define the SiN_x. The desired deposition and patterning routine shown in figure 2 can be continued until all thicknesses of compressive film are met. Note that all patterns were the same dimension; therefore, larger radii micro-tubes only have $\frac{3}{4}$'s of a turn (figure 2.5j) or $\frac{1}{2}$ of a turn (figure 2.5k). The LF-SiN_x layers in figure 2.5i-k total in thickness of 25nm, 35nm, and 55nm, respectively, yielding 6, 6.8, and 9.5 μ m. These diameters are larger than predicted most likely due to the interaction of the plasma with the Mg film, forming MgF and reducing the adhesion of SiN_x during plasma deposition. It is also possible that removing the sample from the PECVD chamber multiple times could result in a film with higher oxynitride formation at the exposed faces and thus less compressive strain.

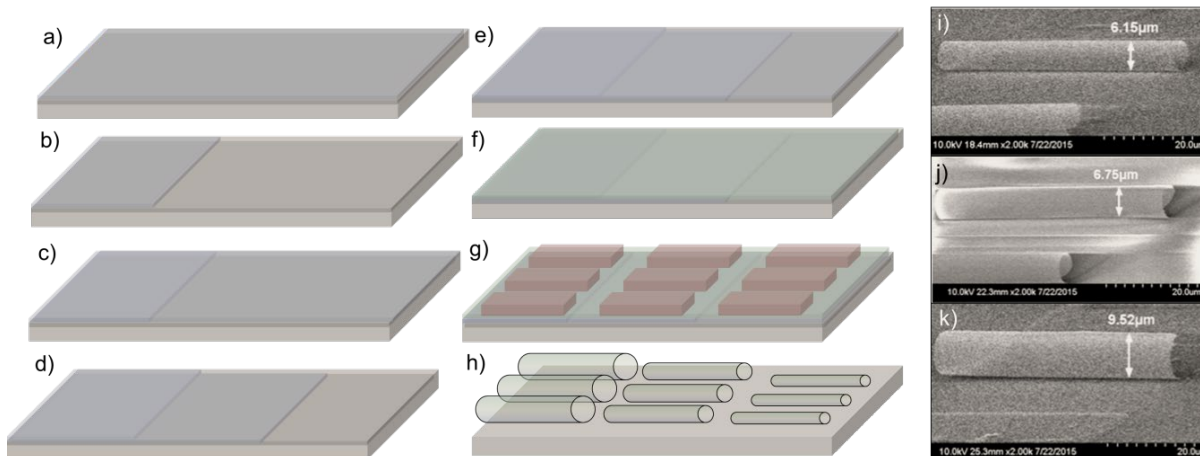


Figure 2. Multi-diameter micro-tubes on single substrate. The fabrication scheme for multi-diameter chips can be seen from (a)-(h): (a) deposition of the compressive layer, (b) patterned etch back of compressive layer, repetition of (a)-(b) until intended number different diameters is formed (c-e), (f) deposition of tensile layer, (g) mesa formation, and (h) sacrificial layer removal. The triple diameter chips are shown through SEM from thinnest bilayer (i) to thickest bilayer (k), and thus smallest and largest diameter micro-tubes, respectively.

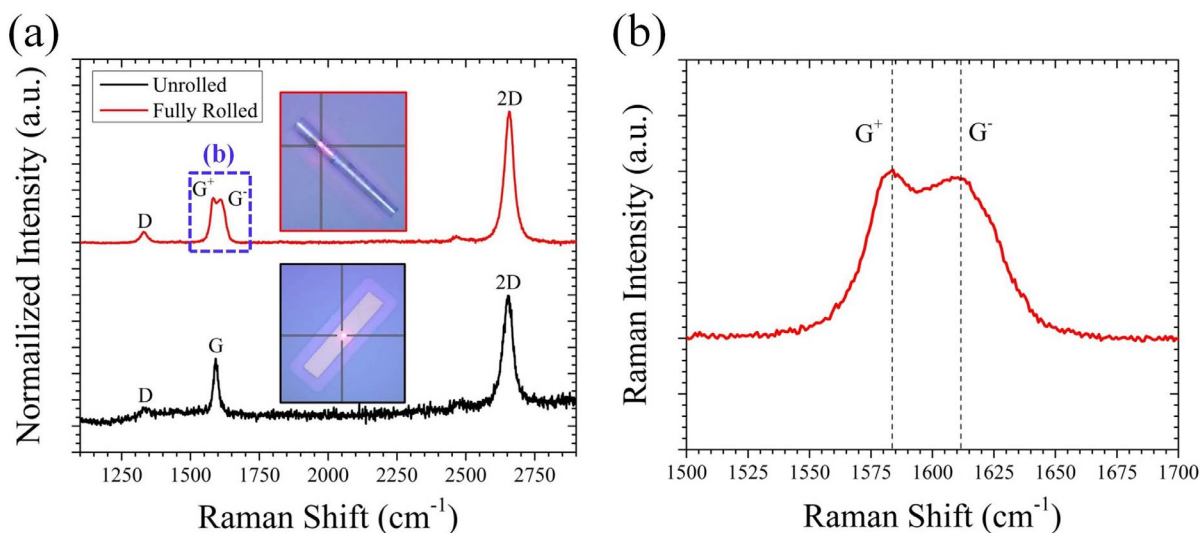


Figure 3. (a) Raman spectra obtained from flat (black curve) and fully rolled (red curve) graphene films. Optical images of the flat (black border) and fully rolled (red border) graphene/SiN_x heterostructured micro-tubes are shown as insets, with the laser excitation spot location denoted by the intersecting cross-hairs. (b) Expanded view of doubly-degenerate G-band of the rolled graphene film, clearly showing the sub-band splitting (indicated by blue, dashed box in (a)).

Strain analysis was carried out after rolling of the graphene/SiN_x micro-tube heterostructures via room-temperature micro-Raman spectroscopy, using a Renishaw inVia microscope system. Upon increasing compressive strain, the doubly degenerate G band of the graphene Raman spectrum becomes split into G⁺ and G⁻ sub-bands, the separation of which allows for quantifiable strain characterization [29]. Figure 3(a) shows representative Raman spectra obtained from flat (black curve) and fully rolled (red curve) graphene films. The graphene Raman signature shows a clear splitting of the G-band in the case of the rolled (compressively strained) foil, whereas no such sub-band signal is detected from the planar graphene sheet. An expanded view of the G-band signature of the strained graphene film is shown in Figure 3(b).

Interestingly, as rolling progresses by extending the duration of the sacrificial layer wet-etching period, the formation of narrower diameter tubes becomes associated with a characteristic increase in the separation of the G⁺ and G⁻ sub-bands of graphene Raman signature. Figure 4(a) plots the position of the G⁺ and G⁻ sub-bands as a function of the micro-tube diameter. Similarly, the micro-tube diameter-dependent G sub-band spacing is plotted in Figure 4(b), with the right-side vertical axis quantifying the resultant compressive strain in the graphene layer, as measured according to the formalism presented by Frank et al. [7].

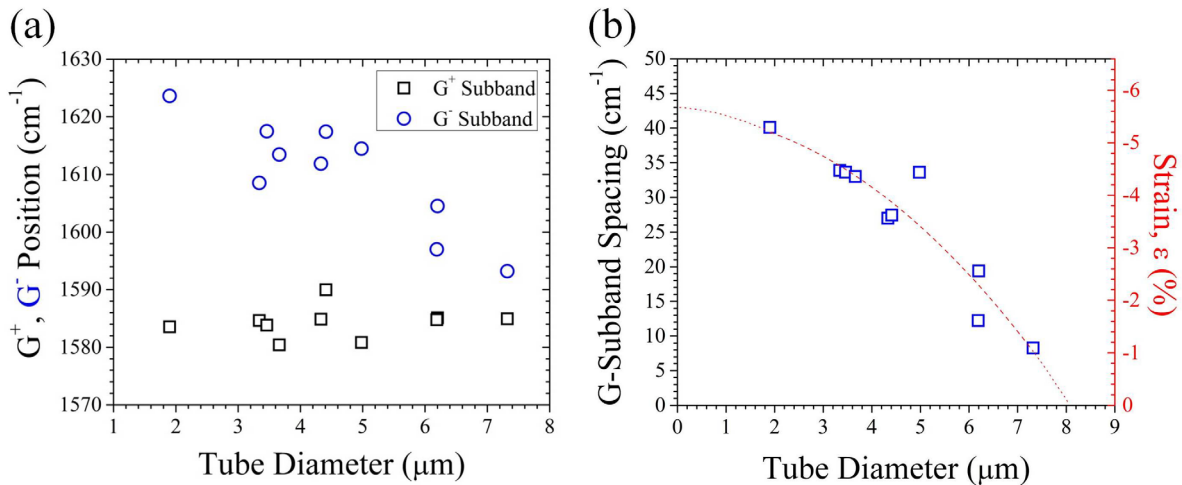


Figure 4. (a) Position of G⁺ and G⁻ sub-bands and (b) G sub-band spacing and graphene strain measured as function of the graphene/SiN_x micro-tube diameter. The red curve in (b) shows a polynomial fit to the data, projected beyond the data set for smaller/larger tubes.

We note that the transferred graphene monolayer is attached to the stressed SiN_x thin film stack by van der Waals force. During the processing steps from transfer to rolling, if the graphene layer is wrinkled or broken, it will not be conformal to the SiN_x surface, hence not be in sync locally with the curvature of the rolled-up SiN_x film stack. We indeed had samples that experienced processing issues and the trend observed in Figure 4 was not observed in those cases.

In summary, across a widely tunable micro-tube diameter range of roughly 1 – 8 microns, we have shown that over 5 % compressive strain can be induced in a mono-layer graphene film via spontaneous rolling in a SiN_x bilayer structure. This work shows an unprecedented range of strain engineering in graphene and holds promise for similar strain control in other two-dimensional materials, such as MoS₂, wherein uniaxial deformation can allow for bandgap energy tunability. The self-rolled, three-dimension heterostructure platform highlighted here has potential for applications in ultra-compact inductors, micro-fluidic channel bio-sensors, rolled-up transistors, and micro-cavity optical resonators.

References:

- [1] Ando T 2009 The electronic properties of graphene and carbon nanotubes *NPG Asia Mater.* 2009 11 **1** 17–21
- [2] Naumis G G, Barraza-Lopez S, Oliva-Leyva M and Terrones H 2017 Electronic and optical properties of strained graphene and other strained 2D materials: a review *Reports Prog. Phys.* **80** 096501
- [3] Castro Neto A H, Guinea F, Peres N M R, Novoselov K S and Geim A K 2009 The electronic properties of graphene *Rev. Mod. Phys.* **81** 109–62
- [4] Choi S M, Jhi S H and Son Y W 2010 Effects of strain on electronic properties of graphene *Phys. Rev. B - Condens. Matter Mater. Phys.* **81** 081407
- [5] Lin K M, Huang Y H, Su W S and Leung T C 2014 Strain effects on the band gap and work function of zigzag single-walled carbon nanotubes and graphene: A comparative study *Comput. Phys. Commun.* **185** 1422–8
- [6] Pereira V M and Castro Neto A H 2009 Strain Engineering of Graphene’s Electronic Structure *Phys. Rev. Lett.* **103** 046801
- [7] Frank O, Tsoukleri G, Parthenios J, Papagelis K, Riaz I, Jalil R, Novoselov K S and Galiotis C 2010 Compression behavior of single-layer graphenes *ACS Nano* **4** 3131–8
- [8] Wang L, Zihlmann S, Baumgartner A, Overbeck J, Watanabe K, Taniguchi T, Makk P and Schönenberger C 2019 In Situ Strain Tuning in hBN-Encapsulated Graphene Electronic Devices *Nano Lett.* **19** 4097–102
- [9] Si C, Sun Z and Liu F 2016 Strain engineering of graphene: a review *Nanoscale* **8** 3207–17
- [10] Ni Z H, Chen W, Fan X F, Kuo J L, Yu T, Wee A T S and Shen Z X 2008 Raman spectroscopy of epitaxial graphene on a SiC substrate *Phys. Rev. B - Condens. Matter Mater. Phys.* **77** 115416
- [11] Spear J C, Custer J P and Batteas J D 2015 The influence of nanoscale roughness and substrate chemistry on the frictional properties of single and few layer graphene

- [12] Deng B, Wu J, Zhang S, Qi Y, Zheng L, Yang H, Tang J, Tong L, Zhang J, Liu Z, Peng H, Deng B, Zhang S, Qi Y, Zheng L, Yang H, Tang J, Tong L, Zhang J, Liu Z, Peng H and Wu J 2018 Anisotropic Strain Relaxation of Graphene by Corrugation on Copper Crystal Surfaces *Small* **14** 1800725
- [13] Ni Z H, Yu T, Lu Y H, Wang Y Y, Feng Y P and Shen Z X 2008 Uniaxial strain on graphene: Raman spectroscopy study and band-gap opening *ACS Nano* **2** 2301–5
- [14] Pérez Garza H H, Kievit E W, Schneider G F and Staufer U 2014 Controlled, reversible, and nondestructive generation of uniaxial extreme strains (>10%) in graphene *Nano Lett.* **14** 4107–13
- [15] Androulidakis C, Koukaras E N, Parthenios J, Kalosakas G, Papagelis K and Galiotis C 2015 Graphene flakes under controlled biaxial deformation *Sci. Reports 2015 51* **5** 1–11
- [16] Prinz V Y, Seleznev V A, Gutakovskiy A K, Chehovskiy A V., Preobrazhenskii V V., Putyato M A and Gavrilova T A 2000 Free-standing and overgrown InGaAs/GaAs nanotubes, nanohelices and their arrays *Phys. E Low-Dimensional Syst. Nanostructures* **6** 828–31
- [17] Chun I S and Li X 2008 Controlled assembly and dispersion of strain-induced InGaAs/GaAs nanotubes *IEEE Trans. Nanotechnol.* **7** 493–5
- [18] Mei Y, Huang G, Solovev A A, Ureña E B, Mönch I, Ding F, Reindl T, Fu R K Y, Chu P K and Schmidt O G 2008 Versatile approach for integrative and functionalized tubes by strain engineering of nanomembranes on polymers *Adv. Mater.* **20** 4085–90
- [19] Froeter P, Yu X, Huang W, Du F, Li M, Chun I, Kim S H, Hsia K J, Rogers J A and Li X 2013 3D hierarchical architectures based on self-rolled-up silicon nitride membranes *Nanotechnology* **24**
- [20] Ma Z, Tian Z, Li X, You C, Wang Y, Mei Y and Di Z 2021 Self-Rolling of Monolayer Graphene for Ultrasensitive Molecular Sensing *ACS Appl. Mater. Interfaces* **13** 49146–52
- [21] Moradi S, Naz E S G, Li G, Bandari N, Bandari V K, Zhu F, Wendrock H and Schmidt O G 2020 Highly Symmetric and Extremely Compact Multiple Winding Microtubes by a Dry Rolling Mechanism *Adv. Mater. Interfaces* **7**
- [22] Dai L and Zhang L 2013 Directional scrolling of SiGe/Si/Cr nanoribbon on Si(111) surfaces controlled by two-fold rotational symmetry underetching *Nanoscale* **5** 971–6
- [23] Yang Z, Kraman M D, Zheng Z, Zhao H, Zhang J, Gong S, Shao Y V, Huang W, Wang P and Li X 2020 Monolithic Heterogeneous Integration of 3D Radio Frequency L–C Elements by Self-Rolled-Up Membrane Nanotechnology *Adv. Funct. Mater.* **30** 1–10
- [24] Songmuang R, Rastelli A, Mendach S, Deneke C and Schmidt O G 2007 From rolled-up Si microtubes to SiOx/Si optical ring resonators *Microelectron. Eng.* **84** 1427–30

- [25] Khandelwal A, Athreya N, Tu M Q, Janavicius L L, Yang Z, Milenkovic O, Leburton J P, Schroeder C M and Li X 2022 Self-assembled microtubular electrodes for on-chip low-voltage electrophoretic manipulation of charged particles and macromolecules *Microsystems Nanoeng.* 2022 81 **8** 1–12
- [26] Huang W, Yang Z, Kraman M D, Wang Q, Ou Z, Rojo M M, Yalamarthy A S, Chen V, Lian F, Ni J H, Liu S, Yu H, Sang L, Michaels J, Sievers D J, Gary Eden J, Braun P V., Chen Q, Gong S, Senesky D G, Pop E and Li X 2020 Monolithic mtesla-level magnetic induction by self-rolled-up membrane technology *Sci. Adv.* **6** 28–30
- [27] Froeter P, Huang Y, Cangellaris O V., Huang W, Dent E W, Gillette M U, Williams J C and Li X 2014 Toward intelligent synthetic neural circuits: Directing and accelerating neuron cell growth by self-rolled-up silicon nitride microtube array *ACS Nano* **8** 11108–17
- [28] Mohseni P K, Behnam A, Wood J D, English C D, Lyding J W, Pop E and Li X 2013 InxGa1-xas nanowire growth on graphene: Van der waals epitaxy induced phase segregation *Nano Lett.* **13** 1153–61
- [29] Mohiuddin T M G, Lombardo A, Nair R R, Bonetti A, Savini G, Jalil R, Bonini N, Basko D M, Galiotis C, Marzari N, Novoselov K S, Geim A K and Ferrari A C 2009 Uniaxial strain in graphene by Raman spectroscopy: G peak splitting, Grüneisen parameters, and sample orientation *Phys. Rev. B - Condens. Matter Mater. Phys.* **79** 205433